A HYBRID METHOD IN DETERMINING SKIN FRICTION FIELDS ON THE SURFACE OF FLYING OBJECTS

The Hung Tran[1,*]

[1]*Faculty of Aerospace Engineering, Le Quy Don Technical University*

Abstract

The study of friction fields on object surfaces plays an important role in fluid mechanics. In this study, a hybrid method, which combines the cross-correlation algorithm and the optical flow algorithm, is developed to calculate the skin-friction field based on the oil distribution on the surface. The scientific basis of the method is presented. Based on this, a computational program is developed and applied to flow calculations over different object surfaces, including an aircraft wing at a high angle of attack, a wing with a low aspect ratio, a delta wing, and the axisymmetric boattail of a flying object. The computational results show that this method effectively determines the flow characteristics of the surface skin-friction field. Flow characteristics, including separation and reattachment locations, are analyzed. Additionally, the influence of computational parameters on the results is specifically presented. This method demonstrates high efficiency and can be applied to future research and aircraft designs.

Keywords: *Cross-correlation algorithm; optical flow; skin-friction field; separation; reattachment.*

1. Introduction

Along with pressure, skin friction is an important parameter in fluid mechanisms. At low velocities, drag generated by skin friction can account for up to 50% of the total drag [1]. Additionally, the skin-friction field allows for the identification of near-surface flow inside the boundary layer of the model. Changes in the direction of the skin-friction field determine the separation and reattachment characteristics of the flow around the model. These characteristics significantly alter the distribution of the pressure field, thereby changing the aerodynamic properties of the model. Accurately predicting skin friction is crucial importance for determining aerodynamic characteristics and flow behavior.

The skin-friction field is typically determined through experimental methods which are divided into point measurement methods and global measurement methods. In point measurement methods, measuring devices are usually placed parallel to the surface [2]. Since they are positioned directly in the measurement region, the actual

[*] Corresponding author, email: tranthehung_k24@lqdtu.edu.vn
DOI: 10.56651/lqdtu.jst.v20.n02.937

measurement values may be altered, leading to reduced measurement accuracy. Furthermore, point measurement methods can only determine friction at specific points on the surface and cannot predict the global field. To overcome this limitation, several global measurement techniques based on image processing have been developed. In these methods, a thin oil layer is applied to the surface. During the experiment, the redistribution of oil occurs due to changes in surface flow phenomena. From the final oil layer distribution, flow phenomena, and quantitative skin friction can be analyzed. Specifically, the flow separation location corresponds to regions where oil highly accumulates while the flow reattachment points correspond to the thinnest oil layer. By incorporating oil distribution data at different time periods, additional methods such as interferometry and optical flow have been developed to determine skin-friction values in the interaction region [3], [4]. Experimental results play a crucial role in providing data for simulation adjustment, leading to the development of various simulation models. In Reynolds-averaged Navier-Stokes models, the boundary layer with a normal distribution function was identified and used [5].

The optical-flow method for determining the skin-friction field was developed by Liu *et al.* [3] in recent years. In this method, the Horn-Schunck scheme is used to determine the initial solution of the problem. This initial solution is then used as input for further calculations in the refined scheme proposed by Liu *et al.* More recently, Tran and Chen developed a new algorithm that allows for the prediction of the skin-friction field using a single scheme [6]. The results of Lin *et al.* and Tran *et al.* have been applied to various typical flow cases such as flow around boattails and flow over the Ahmed body surface [7], [8]. However, both methods require multiple iterations to approximate the skin-friction field. Using excessive iterations can overly smooth small-scale features of the flow and thereby introduce significant errors. Additionally, the computational time for a single case is taken long with high computer resources. An improvement technique is required to obtain the accurate results in a suitable time.

In this study, the author proposes a hybrid algorithm for calculating the skin-friction field around flying objects to overcome the limitation of previous ones. Specifically, in the first step, the cross-correlation algorithm is used to compute a low-resolution skin-friction field. Then, the method developed by Tran and Chen is applied, using the initial skin-friction results obtained from the cross-correlation method. The use of Tran and Chen's scheme enhances the resolution of the skin-friction field while improving the physical significance of the flow phenomenon. Meanwhile, using the initial results from the cross-correlation method helps reduce computational time. The details of the algorithm, its advantages and disadvantages, and its application to several

typical models, including wing, delta wings, and boattail models will be presented in Section 2 and Section 3 of this article. This study indicates that the current method provides sufficiently accurate results of the skin-friction fields. The typical flow features including separation and reattachment positions will be discussed.

2. Methodology and experimental setup

2.1. The hybrid method in determining skin-friction fields

The hybrid algorithm is used for calculating the skin-friction field. This algorithm determines the skin-friction field through two stages: first, it calculates a low-resolution skin-friction field using the cross-correlation algorithm. Then, it applies the results of the cross-correlation method and the algorithm developed by Tran and Chen [6] to produce a high-resolution skin-friction field.

The cross-correlation algorithm is typically used for discrete image data. In this method, data from two image pairs are utilized for computation. In each image, the data is divided into small interrogation windows with sizes of 8 × 8 pixels or larger. The displacement of an interrogation window in the first image compared to the second image is computed using the cross-correlation method. From this, the two velocity components can be determined based on the displacement and the time interval between the two images. The cross-correlation method has been commonly used in previous studies for velocity analysis in particle image velocimetry (PIV) measurement [9], [10]. The primary advantage of this method is its low sensitivity to image noise and its relatively accurate determination of the displacement. However, using interrogation windows reduces the resolution of the velocity field. Specifically, the velocity field resolution can decrease by up to 64 times compared to the original image. Interpolation and extrapolation methods can be applied to increase the velocity field size to match the original image, but the improvement in resolution is minimal. Furthermore, in the cross-correlation method, interrogation windows are processed independently whereas fluid displacement is continuous in reality. As a result, this approach may reduce the physical meaning of the results. Additionally, the method is less effective for images with continuously varying brightness such as oil flow images, making it less commonly used in previous studies for skin-friction analysis. However, since this method can reduce the noise of measurement highly, initial results are sufficient for further estimation.

To improve the accuracy of the skin-friction field, the author proposes using a hybrid method. Specifically, the results from the cross-correlation method are interpolated to match the original image size. These data are then used as the initial results for calculations using the optical-flow method. The optical-flow method is

applied similarly to the approach presented by Tran and Chen [6]. In this method, the initial optical-flow vectors are zeros and they are steadily improved after each iteration. However, the process takes a high number of iteration. Additionally, in some cases, the results are not converged. Consequently, initial results are important for the estimation process. By using the initial results from the cross-correlation method, the convergence process is much faster, and the number of required iteration is reduced. This is the most advantage of the hybrid method. Additionally, the author proposes using a fixed Lagrange constant for both divergence and vorticity magnitude to simplify the calculation process. The detailed approach is as follows:

First, the skin-friction field is computed using the optical-flow method based on the following equation:

$$\frac{\partial h}{\partial t}+\nabla\left[\frac{h^2\boldsymbol{\tau}_w}{2\mu}-\left(\nabla p-\rho\,\boldsymbol{g}\right)\frac{h^3}{3\mu}\right]=0 \tag{1}$$

where $\boldsymbol{\tau}$ is the two-component skin-friction vector, h oil layer thickness, ρ density of the oil, p pressure on the surface and $\boldsymbol{g}$ is the gravity vector. In the above equations, the pressure and density components are typically omitted from calculations, as they are much smaller compared to the other two components [3], [7]. In the optical-flow method, the thickness of the oil layer is considered proportional to the intensity of the pixel brightness [11], [12]. Through pre-experiment calibration, this relationship can be established. Based on these assumptions, Eq. (1) transforms into:

$$\frac{\partial I}{\partial t}+\nabla\left(I\boldsymbol{u}\right)=0 \tag{2}$$

where vector $\boldsymbol{u}$ is determined as follows:

$$\boldsymbol{u}=\frac{\kappa I}{2\mu}\boldsymbol{\tau} \tag{3}$$

Typically, the brightness intensity obtained from images is affected by noise. To reduce this, Tran and Chen proposed using a Gaussian filter for (2). Additionally, the equation is solved using the variational method. Specifically, the variational function for vector $\boldsymbol{u}$ has the following form:

$$J(\overline{\boldsymbol{u}})=\int_{\Omega}\left[\overline{u}\,\overline{I}_x+\overline{v}\,\overline{I}_y+\overline{I}_t-D_t\Delta\overline{I}\right]^2dxdy+\alpha\int_{\Omega}\left[\left(\overline{u}_x+\overline{v}_y\right)^2+\left(\overline{u}_y-\overline{v}_x\right)^2\right]dxdy \tag{4}$$

where D_t is the turbulent diffusion coefficient and it depends on $\boldsymbol{u}$, α is Lagrange coefficient [13]. The overline denotes values that have been filtered using the Gaussian

filter. The variational function (4) is optimized using the Euler-Lagrange method, allowing the vectors $\boldsymbol{u}$ and $\boldsymbol{\tau}$ to be determined. In detail, the Euler-Lagrange equations for $J(\bar{\boldsymbol{u}})$ can be written as:

$$\frac{\partial J(\bar{\boldsymbol{u}})}{\partial \bar{\boldsymbol{u}}} - \frac{\partial}{\partial \boldsymbol{x}} \frac{\partial J(\bar{\boldsymbol{u}})}{\partial \bar{\boldsymbol{u}}'} = 0 \tag{5}$$

Adding $J(\bar{\boldsymbol{u}})$ from (4) to (5) leads to:

$$\begin{aligned} \bar{I}_x \left(\bar{I}_t + \bar{u}\bar{I}_x + \bar{v}\bar{I}_y + D_t \Delta \bar{I} \right) &= \alpha \left(\bar{u}_{xx} + \bar{v}_{xy} + \bar{u}_{yy} - \bar{v}_{xy} \right) \\ \bar{I}_y \left(\bar{I}_t + \bar{u}\bar{I}_x + \bar{v}\bar{I}_y + D_t \Delta \bar{I} \right) &= \alpha \left(\bar{v}_{yy} + \bar{u}_{xy} + \bar{v}_{xx} - \bar{u}_{xy} \right) \end{aligned} \tag{6}$$

Making discrete equation by time and space, the velocity at iteration $n + 1$ can be found from n by the below equations:

$$\begin{pmatrix} \bar{u}^{n+1} \\ \bar{v}^{n+1} \end{pmatrix} = \alpha \begin{pmatrix} \bar{I}_x^2 + 2\alpha \left(\frac{1}{h^2} + \frac{1}{h^2} \right) & \bar{I}_x \bar{I}_y \\ \bar{I}_x \bar{I}_y & \bar{I}_y^2 + 2\alpha \left(\frac{1}{h^2} + \frac{1}{h^2} \right) \end{pmatrix}^{-1} \cdot \begin{pmatrix} \left(\bar{u}_1^n + \bar{u}_2^n \right) \bar{I}_y^2 + 4\alpha \left(\bar{u}_1^n + \bar{u}_2^n \right) - 4\alpha \bar{I}_x \left(\bar{I}_t + D_t \Delta \bar{I} \right) - \bar{I}_x \bar{I}_y \left(\bar{v}_1^n + \bar{v}_2^n \right) \\ \left(\bar{v}_1^n + \bar{v}_2^n \right) \bar{I}_x^2 + 4\alpha \left(\bar{v}_1^n + \bar{v}_2^n \right) - 4\alpha \bar{I}_y \left(\bar{I}_t + D_t \Delta \bar{I} \right) - \bar{I}_x \bar{I}_y \left(\bar{u}_1^n + \bar{u}_2^n \right) \end{pmatrix} \tag{7}$$

where h is a spatial step, $\bar{u}_1^n = \bar{u}_{xx}^n + \bar{v}_{xy}^n + 2\frac{\bar{u}^n}{h^2}$, $\bar{u}_2^n = \bar{u}_{yy}^n - \bar{v}_{xy}^n + 2\frac{\bar{u}^n}{h^2}$, $\bar{v}_1^n = \bar{v}_{yy}^n + \bar{u}_{xy}^n + 2\frac{\bar{v}^n}{h^2}$, and $\bar{v}_2^n = \bar{v}_{xx}^n + \bar{u}_{xy}^n + 2\frac{\bar{v}^n}{h^2}$.

Clearly, when the initial values of optical-flow vectors are known, the results at the next interaction can be found faster and the number of the initial interaction reduces. In this study, the maximum iteration is selected at n = 10. Note that since the initial results are obtained from the cross-correlation algorithm, the requirement of total error for convergence of the solutions is not required, as shown by the optical-flow algorithm.

The vector $\boldsymbol{u}$ is found by an iteration methods. The computational steps and discretization process are described in [6], [14]. As mentioned earlier, the initial values obtained from the cross-correlation method are used, reducing the number of iterations in the calculations. Additionally, the optical-flow method considers neighboring points when computing derivatives and differentials, ensuring continuity. This method enables

the calculation of the skin-friction field from a single image pair. By averaging the results over different time periods, the mean skin-friction field can be determined. A MATLAB program has been developed to implement the algorithm. Although the hybrid method shows an advantage for estimation, some small-scale features can be removed due to using initial results from cross-correlation methods. Detailed experimental setup and results will be presented in the next sections. Note that the method uses an assumption of the linear relation between the thickness of the oil and its intensity. However, this assumption is not always satisfied in separation regions where the oil is highly accumulated. A pre-calibration process should be conducted before calculation to obtain the quantitative skin-friction fields. Additionally, the selection of oil images for the data processing should be evaluated for the accuracy of the results.

2.2. Experimental setup and data collections

Experiments for determining the skin-friction field using the optical-flow method are generally similar, with differences mainly in the type of luminescent oil substance and the parameters of the measurement devices. A typical experimental setup for measuring the skin-friction field is illustrated in Fig. 1. Typically, the experiment consists of a camera and LED lights. The camera is positioned above the model, ensuring that its sensor is parallel to the measurement surface. LED lights are placed on both sides to provide uniform illumination. Before the experiment, a uniform layer of luminescent oil is applied to the model's surface. During the experiment, the oil layer moves and changes in thickness which alters the brightness intensity of the images. The camera records these changes in reflected brightness from the oil layer, facilitating data processing and calculations in subsequent steps (as discussed in Section 2.1). The selection of an appropriate luminescent oil plays a crucial role in the experiment. Generally, above twenty image pairs are sufficient to obtain the average global skin-friction fields.

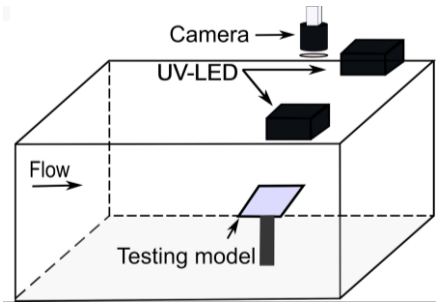

Fig. 1. Experimental setup for skin-friction measurement.

3. Results and discussions

3.1. Skin-friction fields around a wing model

In this section, the results of the skin-friction field over an aircraft wing surface are analyzed. Additionally, the influence of computational parameters on the results is presented to evaluate the effectiveness of the method in determining the surface flow field of the model. The angle of attack in this case is 18° for clearly identifying flow separation and other flow characteristics. The oil is a substance of silicon oil and UV dye (Petroleum Tracer Concentrate DFSB-K175). The speed of the wind tunnel was 20 m/s giving a Reynolds number based on the chord length of the wing at $Re = 1.7 \cdot 10^5$. The frame rate of the camera was set at 25 frames per second. To determine the skin-friction field on the aircraft wing, thirty-one pairs of images were used. Each image pair provides the instantaneous friction field at a specific moment. An example of an image pair used for friction field calculations is shown in Fig. 2. Here, the images are stored in an 8-bit with values ranging from 0 to 255.

The results indicate significant changes in brightness intensity on the surface between the two images. Based on these brightness variations, the cross-correlation and optical-flow methods can be applied to calculate the skin-friction field. The results from the two images also reveal an accumulation of oil near the center of the model, around the position $x/C = 0.4$. This oil accumulation corresponds to the position of the separation flow, as commonly analyzed in previous studies [6].

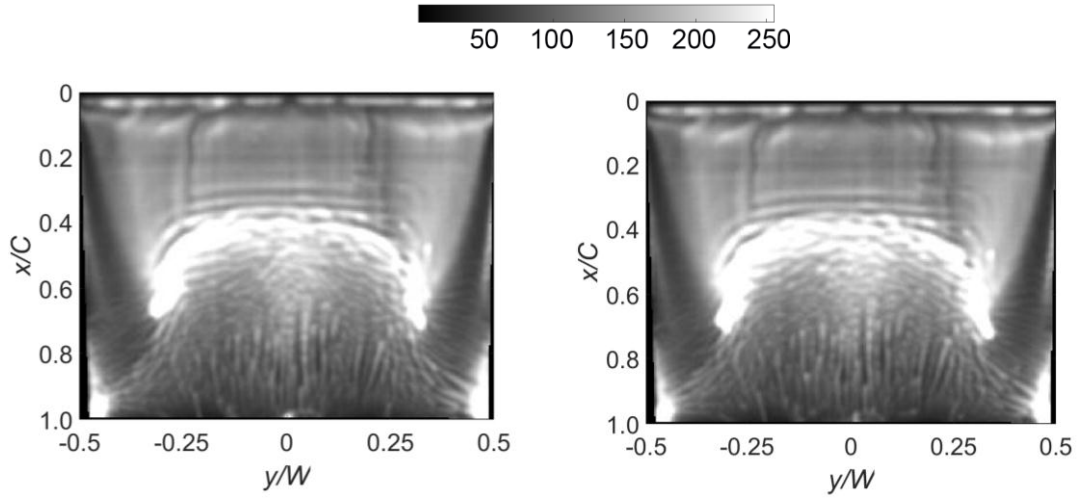

a) The first image *b) The second image*

Fig. 2. An example of two images used for calculation.

More specifically, Fig. 3 illustrates the near-surface streamlines of the model based on the calculated friction field. This flow field is overlaid on the final luminescent oil image on the surface. It should be noted that the flow was often discussed in previous studies based on the distribution of the last oil image. Consequently, the oil image provides good data to evaluate the results of the algorithm from data processing. A near central flow separation location on the model's surface is clearly visible in the skin-friction field results. It can be observed that the flow separation occurs ahead of the oil accumulation region. Due to the side effect, this separation line has a C-shape, with smaller separations forming at the outer edges.

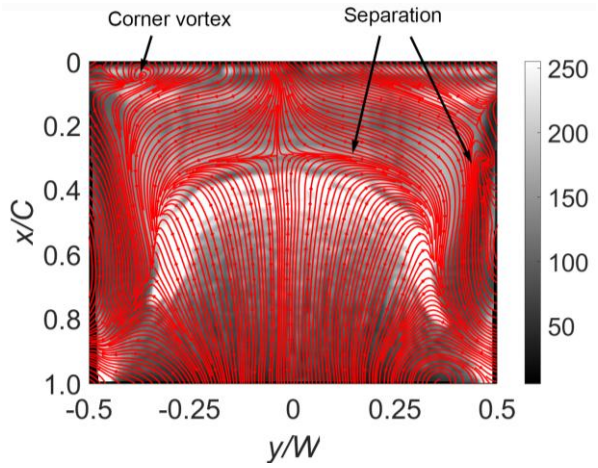

Fig. 3. The skin-friction streamlines and luminescent image.

The reverse flow region occupies up to two-thirds of the entire wing. At high angles of attack, flow separation appears on the wing, leading to a reduction in lift and an increase in drag. Unlike the oil distribution results, a secondary separation line appears at the outer edges of the wing. This phenomenon is due to the wing's low aspect ratio. The pressure difference between the upper and lower surfaces of the wing causes the formation of two vortex sheets running along the wing's outer edges. This behavior is similar to the flow over a delta wing, which will be discussed in later sections. The results demonstrate that the current method provides quantitative insights into the flow field and reveals certain flow characteristics that traditional methods cannot capture. The movement of oil plays a crucial role in accurately analyzing surface flow phenomena. Additionally, using luminescent oil instead of solid powder mixed with oil enhances the accuracy of flow analysis.

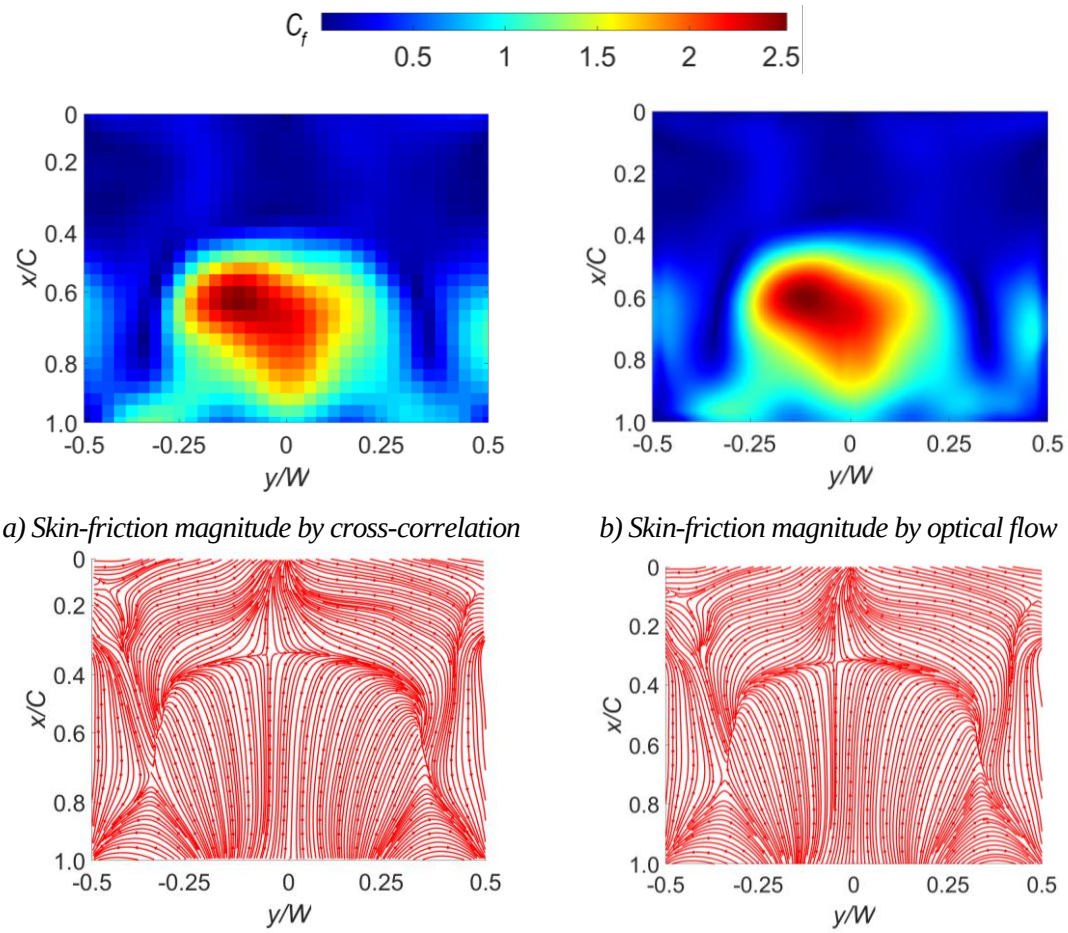

a) Skin-friction magnitude by cross-correlation *b) Skin-friction magnitude by optical flow*

c) Skin-friction streamlines by cross-correlation *d) Skin-friction streamlines by optical flow*

Fig. 4. Comparison of the skin friction by two methods.

Next, Fig. 4 presents the results of the magnitude of the skin-friction field and surface flow on the wing using two methods: cross-correlation and hybrid methods. The results show that the magnitude of the skin-friction field and surface flow are similar between the two methods. However, due to the spatial continuity between points in the computational domain, the hybrid method more clearly represents the physical meaning of the flow. Additionally, the resolution of the skin-friction field is significantly improved using this method, as shown in Fig. 4a, 4b. Here, the resolution of the skin-friction vector in the measurement plane increases 64 times, in comparison to the cross-correlation algorithm. Another important observation is that the cross-correlation method is typically used for images with discrete bright points. However, the method has also shown high effectiveness when the bright points of the image are continuously distributed. This is due to the appropriate time interval selection between the two images and the smooth and consistent movement of the oil on the surface.

Table 1 estimates the numerical time for each algorithm. The numerical process is used by a MATLAB program. A computer with a CPU of Core i7-6820HQ is used for testing. For the optical-flow algorithm, the number of iterations is often from 200 to 1000 for the convergence of the results while the interaction of the hybrid is much lesser. Clearly, the hybrid method allows to reduction of numerical time remarkably, which is suitable for the initial estimation of the experimental process. This can be explained by the fact that the number of iterations in the hybrid method is significantly reduced while still ensuring the convergence of the results.

Tab. 1. Numerical time by different algorithms for a pair image

Algorithm	**Cross-correlation**	**Optical-flow**	**Hybrid**
Numerical time (s)	1.3517	11.1315	1.9886

3.2. Effect of Lagrange coefficient on the results

Since (2) contains two unknown components, a multi-solution state occurs. In fact, the solution depends on the Lagrange coefficient. Therefore, it is necessary to examine the influence of the Lagrange coefficient on the computational results. In this section, calculations are conducted with Lagrange values ranging from 20 to 200000. The calculation is similar in Section 3.1, except for changing the Lagrange coefficients.

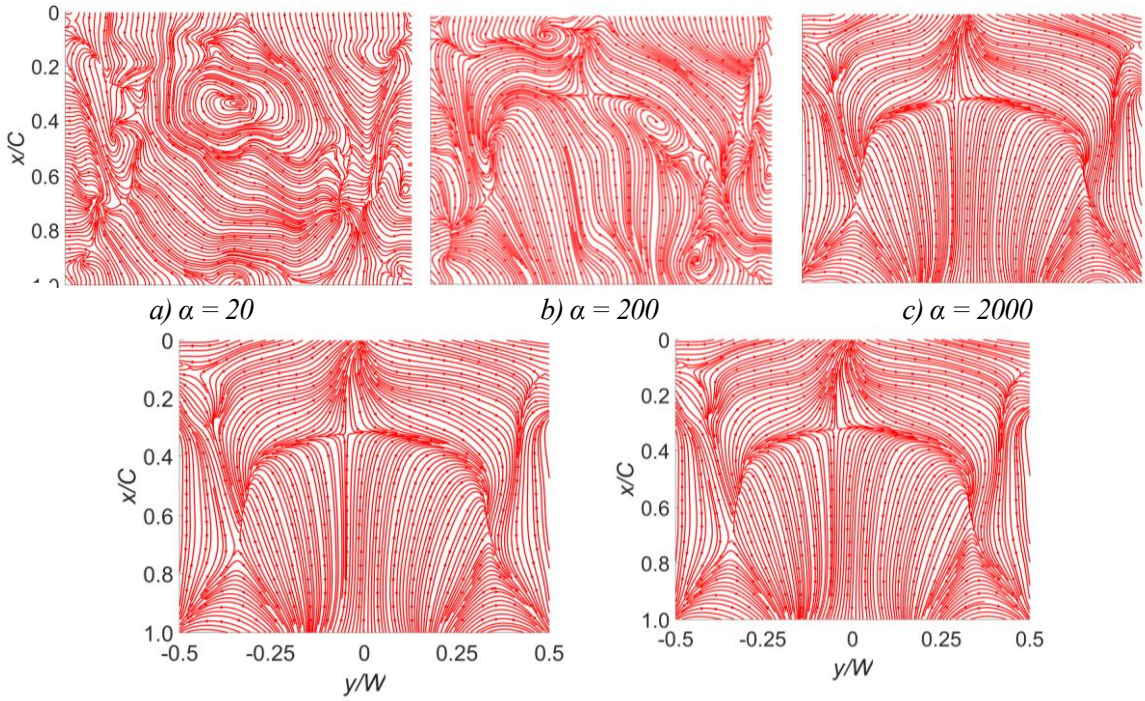

a) α = 20 *b) α = 200* *c) α = 2000*

d) α = 20000 *e) α = 200000*

Fig. 5. Skin-friction streamlines at different Lagrange coefficients.

The results are shown in Fig. 5. The computational results indicate that when the Lagrange coefficient is low, the surface flow is not consistent with the distribution of the oil layer on the surface. Convergence occurs when the Lagrange coefficient exceeds 2000, with minimal changes as the parameter continues to increase. It is evident that selecting an appropriate minimum Lagrange coefficient plays a crucial role in ensuring accurate computational results. The method for determining the minimum Lagrange coefficient is based on comparisons with experimental oil layer distributions. This approach is similar to previous studies by Tran *et al.* [1], [8]. Note that the error of the optical-flow algorithm can increase with a high Lagrange coefficient as shown by Tran *et al.* However, the skin-friction fields by the hybrid method show stability for the Lagrange coefficient above 2000. This is another advantage of the current method.

3.3. Skin-friction fields in a low aspect-ratio wing

Next, the distribution of the skin-friction field on a low-aspect-ratio wing (AR = 0.5) is analyzed at a high angle of attack. The experimental setup and oil substance are similar to the previous case in Section 3.1. The experiments were also conducted in a low-speed wind tunnel. Fig. 6 presents the oil layer distribution in the final image and the surface streamlines. It should be noted that, compared to the previous case, the oil layer is significantly thicker in this scenario. The thick luminescent oil can be visible from the oil distribution after the experimental process. However, it can be observed that the hybrid method provides good results for the surface streamline distribution. Specifically, the separation point appears at x/C = 0.2 and has a circular shape similar to the previous case. However, unlike the previous case, the reattachment point appears at x/C = 0.8, forming a separation-reattachment region on the wing surface. On both edges of the wing, secondary streamlines emerge due to the pressure difference between the upper and lower surfaces of the wing. The streamline results align with the surface pressure distribution, indicating that the hybrid method provides accurate results for surface flow.

3.4. Skin-friction fields on a delta wing

In another case, the flow over a delta wing was analyzed using a hybrid method. In this case, the oil is mixed with UV powders and silicone oil of 200 cSt [15] with an initial thickness of around 20 μm. The experiments were conducted in a low-speed wind tunnel with a test section of around 0.4 × 0.4 m^2 at Western Michigan University. The

velocity of the wind tunnel was 20 m/s and the frame rate of the camera was set at 25 frames per second. It should be noted that in this model, the oil layer undergoes significant changes with a high viscosity, and the fluorescent powder used differs from the previous cases.

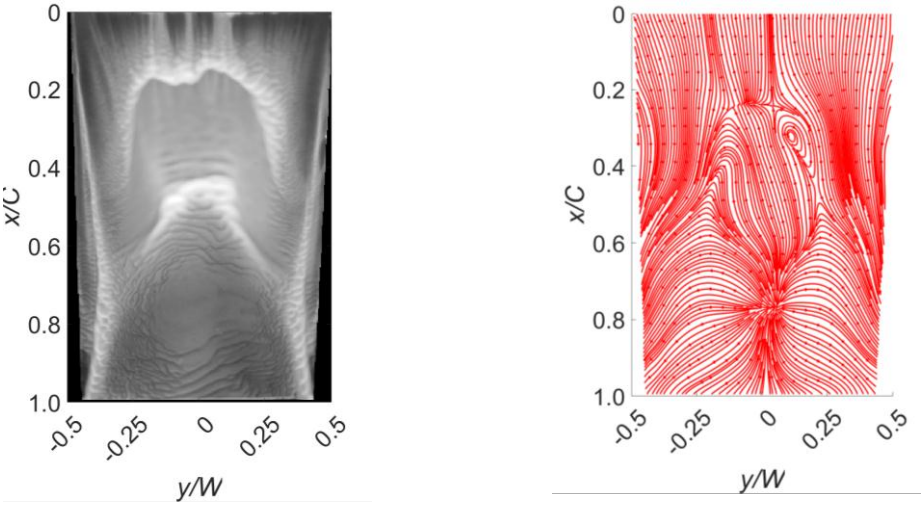

a) Luminescent oil image *b) The skin-friction streamlines*

Fig. 6. Skin friction for wing with AR = 0.5.

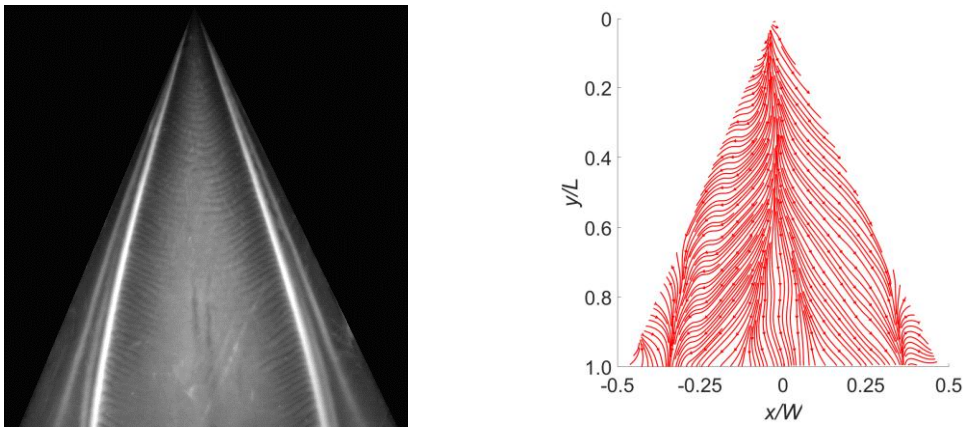

a) Luminescent oil image *b) The skin-friction streamlines*

Fig. 7. Skin friction for delta wing.

Figure 7 presents the oil layer distribution in the final image and the skin-friction field calculated using the hybrid method. It can be observed that the two outer edges of the wing exhibit separation lines. This is due to the formation of small vortex strips at the outer edges, running from the leading edge to the trailing edge of the wing. The

results of the hybrid method are consistent with previous calculations presented by Liu *et al.* [15]. However, minor differences also appear, as the secondary separation line is not observed using the hybrid method. This is because the cross-correlation method has a low resolution for the skin-friction field. As a result, this friction field cannot be reconstructed using the optical-flow method in the later calculation stage. Nevertheless, the main flow characteristics can still be obtained from this method.

3.5. Skin-friction fields around a boattail model

Finally, the hybrid method was applied to the flow around the tail of a rotationally symmetric flight model. The experiment was conducted by Tran *et al.* [1] at Tohoku University, Japan. In this case, the boattail angle is 18°. The oil used is a mixture of oleic acid solvent and fluorescent powder chloro-9,10-bis(phenylethynyl)-anthracene ($C_{30}H_{17}Cl$), with an average viscosity of 27.62 cSt. The velocity of the wind tunnel was set at 37 m/s. The flow results are presented in Fig. 8. Here, the flow direction is from left to right. The oil distribution results indicate that a separation line appears in the transition region between the body and the boattail. The hybrid method accurately describes this line. Additionally, a convergence region forms further downstream of the model. Although this region is difficult to observe from the oil layer, it can be clearly distinguished from the computational results. The results are almost identical to the previous study for a similar boattail model.

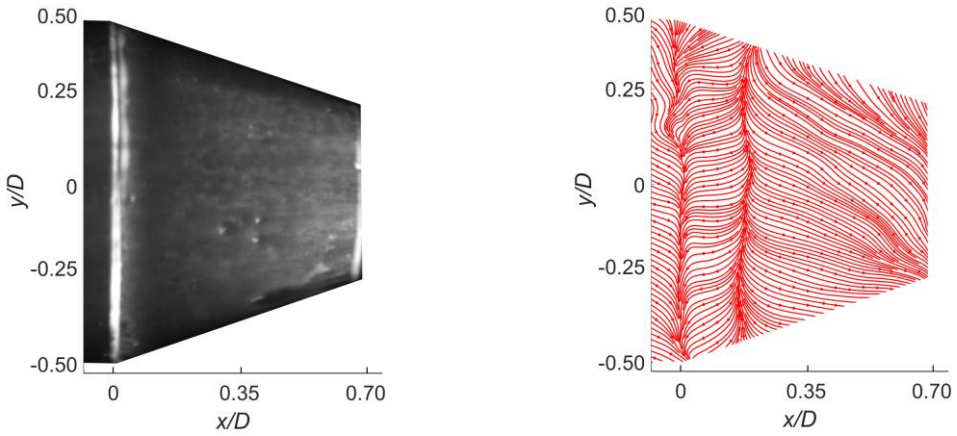

a) Luminescent oil image *b) The skin-friction streamlines*

Fig. 8. Skin friction for 18° boattail model.

Experimental results with different models show that the hybrid method effectively describes the skin friction field and near-surface flow. The main flow features can be captured using this method with relatively few iterations. The

computational results show good agreement with data from previous studies. However, due to the low resolution of the cross-correlation method, some small-scale features of the flow may be difficult to capture. It should be noted that image-processing methods for friction field analysis have been commonly used in recent studies [16]-[19]. The error of this method is approximately 12%, as indicated in previous studies [20], [21]. Since a similar approach is used in this study, the error is expected to be of a similar magnitude. However, to accurately measure the error, an experimental setup and experimental scheme must be conducted. Since the skin friction is often low, this process is complicated. In the author's literature review, there were no studies to evaluate the uncertainty of the skin friction measurement in detail. This remains one of the key objectives of the author's future research. Additionally, it should be noted that the results of the hybrid algorithm were compared with an oil image to evaluate the ability of the method in determining skin friction vectors. Detailed comparison of the measurement errors among optical-flow, cross-correlation, and hybrid methods will be focused on in further studies.

4. Conclusion

The study proposes a hybrid method for calculating the skin friction field on the surface of a moving object. This method combines the cross-correlation algorithm and the optical flow algorithm in computation.

The results indicate that the skin-friction field, with key characteristics such as separation and reattachment positions, can be obtained using the hybrid method. The method demonstrates high efficiency in flow calculations by reducing remarkably numerical time in comparison to the optical-flow algorithm. Additionally, the resolution of the skin-friction fields by the hybrid method improves in comparison to that of the cross-correlation method. For an aircraft wing model at a high angle of attack, a C-shaped separation line appears on the surface. The separation and reattachment regions are also observed on the tail model of a rotationally symmetric object. Meanwhile, outer edge vortices are significant features for low-aspect-ratio and delta wings.

The small Lagrange coefficient in the optical-flow algorithm affects the results. However, with a determined value, the results of the calculation process converge.

Therefore, this parameter needs to be checked carefully by comparison of the skin-friction results with the oil flow distribution before applying it to specific calculations.

Although a hybrid method was proposed in the current study for skin-friction fields, a details evaluation of the uncertainty should be conducted. Additionally, the ability of the method to determine unsteady skin friction should be considered for further investigation. Synthetic images with solutions should be also developed to evaluate the uncertainty among algorithms for skin-friction measurements.

Acknowledgment

The author would like to thank Prof. Keisuke Asai, Prof. Nonomura at Tohoku University, and Prof. Tianshu Liu at Michigan University for their data support.

This research is funded by Le Quy Don Technical University Research Fund under the grant number 24.1.34.

References

[1] T. H. Tran *et al.*, "Effect of boattail angles on the flow pattern on an axisymmetric afterbody surface at low speed", *Experimental Thermal and Fluid Science*, Vol. 99, No. May, pp. 324-335, 2018. DOI: 10.1016/j.expthermflusci.2018.07.034

[2] S. A. Woodiga, "*Global skin friction diagnostics: The GLOF technique and measurements of complex separated flows*", Ph.D. thesis, Western Michigan University, 2013.

[3] T. Liu *et al.*, "Global luminescent oil-film skin-friction meter", *AIAA Journal*, Vol. 46, No. 2, pp. 476-485, 2008. DOI: 10.2514/1.32219

[4] S. A. Woodiga and T. Liu, "Skin friction fields on delta wings", *Experiments in Fluids*, Vol. 47, No. 6, pp. 897-911, 2009. DOI: 10.1007/s00348-009-0686-6

[5] T. H. Tran *et al.*, "Effect of boattail angle on near-wake flow and drag of axisymmetric models: A numerical approach", *Journal of Mechanical Science and Technology*, Vol. 35, No. 2, pp. 563-573, Feb. 2021. DOI: 10.1007/s12206-021-0115-1

[6] T. H. Tran and L. Chen, "Wall shear-stress extraction by an optical flow algorithm with a sub-grid formulation", *Acta Mechanica Sinica/Lixue Xuebao*, Vol. 37, No. 1, pp. 65-79, 2021. DOI: 10.1007/s10409-020-00994-9

[7] T. H. Tran *et al.*, "Deflector effect on flow behavior and drag of an Ahmed body under crosswind conditions", *Journal of Wind Engineering and Industrial Aerodynamics*, Vol. 231, 2022. DOI: 10.1016/j.jweia.2022.105238

[8] T. H. Tran *et al.*, "Effect of Reynolds number on flow behavior and pressure drag of axisymmetric conical boattails at low speeds", *Experiments in Fluids*, Vol. 60, No. 3, pp. 1-19, 2019. DOI: 10.1007/s00348-019-2680-y

[9] V. Gentile *et al.*, "Afterbody effects on axisymmetric base flows", *Journal of Aircraft*, Vol. 53, No. 4, pp. 2285-2294, 2016. DOI: 10.2514/1.J054733

[10] T. H. Tran, "The effect of boattail angles on the near-wake structure of axisymmetric afterbody models at low-speed condition", *International Journal of Aerospace Engineering*, Vol. 2020, Iss. 1, 2020. DOI: 10.1155/2020/7580174

[11] T. T. Hung *et al.*, "Effect of a short, bio-mimetic control device on aerodynamic drag of Ahmed body", *Journal of Fluids Engineering*, Vol. 145, No. 3, 2023. DOI: 10.1115/1.4056341

[12] T. Liu *et al.*, "Skin friction and surface optical flow in viscous flows", *Physics of Fluids*, Vol. 34, No. 6, 2022. DOI: 10.1063/5.0095416

[13] X. Chen *et al.*, "Optical flow for incompressible turbulence motion estimation", *Experiments in Fluids*, 56, pp. 1-14, 2015. DOI: 10.1007/s00348-014-1874-6

[14] T. T. Hung *et al.*, "Experimental study of the skin-friction topology around the Ahmed body in cross-wind conditions", *Journal of Fluids Engineering*, Vol. 144, No. 3, 2022. DOI: 10.1115/1.4052418

[15] T. Liu *et al.*, "Global skin friction diagnostics in separated flows using luminescent oil", *Journal of Flow Visualization and Image Processing*, Vol. 16, No. 1, pp. 19-39, 2009. DOI: 10.1615/JFlowVisImageProc.v16.i1.20

[16] T. Liu, "Global skin friction measurements and interpretation", *Progress in Aerospace Sciences*, Vol. 111, No. October, 2019. DOI: 10.1016/j.paerosci.2019.100584

[17] T. Liu *et al.*, "Skin friction fields and surface dye patterns on delta wings in water flows", *Journal of Fluids Engineering*, Vol. 137, No. 7, pp. 1-14, 2015. DOI: 10.1115/1.4030041

[18] T. Lee *et al.*, "Unsteady skin-friction field estimation based on global luminescent oil-film image analysis", *Journal of Visualization*, Vol. 23, No. 5, pp. 763-772, 2020. DOI: 10.1007/s12650-020-00661-y

[19] N. M. Husen *et al.*, "Luminescent oil film flow tagging skin friction meter applied to FAITH hill", *AIAA Journal*, Vol. 56, No. 10, pp. 3875-3886, 2018. DOI: 10.2514/1.J057114

[20] T. Liu and J. P. Sullivan, "Luminescent oil-film skin-friction meter introduction", *AIAA Journal*, Vol. 36, No. 8, pp. 1460-1465, 1998. DOI: 10.2514/2.538

[21] R. Thibault and G. J. Poitras, "Uncertainty evaluation of friction velocity measurements by oil-film interferometry", *Journal of Fluids Engineering*, Vol. 139, No. 5, 2017. DOI: 10.1115/1.4035461

PHƯƠNG PHÁP LAI TRONG XÁC ĐỊNH TRƯỜNG MA SÁT TRÊN BỀ MẶT VẬT THỂ BAY

Trần Thế Hùng[1]

[1]*Khoa Hàng không Vũ trụ, Trường Đại học Kỹ thuật Lê Quý Đôn*

Tóm tắt: Nghiên cứu trường ma sát trên bề mặt vật thể có vai trò quan trọng trong cơ học chất lưu. Trong nghiên cứu này, phương pháp lai, là sự kết hợp của thuật toán tương quan chéo và thuật toán quang thông, được phát triển trong tính toán trường ma sát từ phân bố dầu trên bề mặt. Cơ sở khoa học của phương pháp được trình bày. Trên cơ sở đó, chương trình tính toán được xây dựng và tính toán cho dòng chảy trên các bề mặt vật thể khác nhau, bao gồm cánh máy bay ở góc tấn lớn, cánh có độ giãn dài nhỏ, cánh tam giác và đuôi vật thể bay dạng đối xứng. Các kết quả tính toán cho thấy phương pháp này xác định tốt đặc trưng dòng chảy của trường ma sát trên bề mặt. Các đặc tính dòng chảy bao gồm vị trí tách hợp dòng được phân tích. Đồng thời ảnh hưởng các tham số tính toán tới kết quả cũng được trình bày cụ thể trong nghiên cứu này. Phương pháp trên cho thấy hiệu quả cao và có thể áp dụng trong nghiên cứu, thiết kế thiết bị bay sau này.

Từ khóa: *Tương quan chéo; quang thông; trường ma sát; tách dòng; hợp dòng.*

Received: 11/02/2025; Revised: 14/05/2025; Accepted for publication: 23/05/2025

❑